Friction **12**(7): 1469–1482 (2024)
https://doi.org/10.1007/s40544-023-0806-y
ISSN 2223-7690
CN 10-1237/TH
RESEARCH ARTICLE

Effects of surface morphology on tribological properties of *Arapaima gigas* scales

Shuaijun ZHANG[1,2], Pengpeng BAI[1], Xiangli WEN[1], Chengwei WEN[1], Hui CAO[1], Wanyou YANG[1], Yu TIAN[1,*]

[1] *State Key Laboratory of Tribology in Advanced Equipment, Department of Mechanical Engineering, Tsinghua University, Beijing 100084, China*

[2] *Key Laboratory of Bionic Engineering (Ministry of Education, China), Jilin University, Changchun 130022, China*

Received: 26 February 2023 / Revised: 12 June 2023 / Accepted: 17 July 2023

Abstract: The remarkable mechanical adaptability of arapaima (*Arapaima gigas*) scales has made them an important subject of study. However, no research has been conducted into their tribological properties, which are crucial for the protectability and flexibility of arapaimas. In this study, by combining morphological characterizations, friction experiments, and theoretical analyses, the relationship between the surface morphology and tribological properties of arapaima scales is determined. These results indicate that arapaima scales exhibit varying surface morphologies in different regions. More specifically, the exposed regions of scales feature grooves and a circulus, whereas the covered regions exhibit bumps. The specific surface morphology of arapaima scales produces varying tribological properties across different regions and sliding directions. The unique tribological properties of arapaima scales influence the forces received from predator attacks and neighboring scales, directly influencing the arapaima's protective capabilities. This study provides new insights into the mechanisms of natural flexible dermal armors, and it has potential applications in personal protective systems.

Keywords: arapaima; scales; surface morphology; tribological properties; protectability

1 Introduction

Through millions of years of evolution, organisms have developed various structures and survival mechanisms. Despite being composed of a limited number of components, biological materials exhibit remarkable functionalities that often surpass those of artificially engineered materials. The remarkable performance of these materials can be attributed to their innovative biological strategies. Comprehensive analyses of biological materials are crucial for the development of high-performance engineering materials. Arapaima (*Arapaima gigas*), an ancient fish species native to the Amazon basin, thrives amidst a hostile environment populated by piranhas. These fearsome predators are renowned for their razor-sharp teeth and formidable predatory nature, posing a mortal threat to various organisms. Nevertheless, the scales of arapaima exhibit an astonishing capacity to withstand piranha attacks while concurrently delivering exceptional flexibility, facilitating agile swimming in water. As a result, the remarkable protection and flexibility displayed by arapaima scales hold promising potential for enhancing battlefield protection for soldiers. In the contemporary battlefield, the paramount considerations for ensuring soldier safety and effectiveness lie in protection and flexibility, particularly in areas such as the neck, elbow, and knee. Unrestricted mobility in these regions is of utmost importance as it plays a pivotal role in enhancing soldiers' survivability in combat situations. Consequently, scientific researchers have devoted significant attention to investigating

* Corresponding author: Yu TIAN, E-mail: tianyu@mail.tsinghua.edu.cn

the remarkable protection and flexibility exhibited by arapaima scales, rendering them a subject of extensive study [1–3]. The scale of arapaima may provide further inspiration for the development of personal protective systems.

Numerous investigations of arapaima scales have been conducted [4–7]. Arapaima scales are primarily composed of both organic and inorganic components, resulting in a multilayer composite material with outstanding mechanical properties. These scales can be divided into two layers: external and internal [8–10]. The external layers of arapaima scales have a high inorganic content and are highly mineralized; this contributes to their high hardness and scale-strengthening effect [11–13]. In contrast, the internal layers of arapaima scales have a high organic content and are less mineralized, resulting in better softness and flexibility [2, 12, 13]. Furthermore, these inner layers contain a significant number of collagen fibers arranged in multiple layers [8, 14, 15]. The collagen fibers within each layer are arranged in parallel; however, the fibers of adjacent layers are oriented at certain angles with respect to each other [16, 17]. This unique structural arrangement further enhances the mechanical adaptability of the scales, by allowing for the deformation and rotation of collagen fibers [18–21]. Moreover, the mechanical properties of arapaima scales are closely related to their moisture content [8, 11, 22]. When arapaima scales are dry, their hardness and elastic modulus increase but their flexibility decreases [23, 24]. Conversely, when wet, their hardness and elastic modulus decrease but their flexibility increases [23, 24]. Studies have indicated that the ridge line and circulus of the arapaima scales play an important role in enhancing their overall damage tolerance [16]. To summarize, arapaima scales are extraordinary materials. These unique characteristics contribute to their protective abilities, enhancing the organism's chances of survival in the face of predator attacks.

It is worth emphasizing that the scales on the body of the arapaima are arranged in an imbricate pattern [25–28]. Hence, the interaction effects of slippage, locking, and support between arapaima scales is a crucial factor influencing the animal's protection during attack. Similarly, these functions are vital for ensuring swimming agility [29–31]. However, none of the studies in the relevant literature have considered these interactions between scales. It is imperative to study the interaction between arapaima scales. For imbricated structures, the tribological properties of scales are crucial factors that influence their inter-scale interactions. However, research into the tribological properties of arapaima scales remains lacking. Hence, this study aims to fill this knowledge gap, by investigating the effects of the scales' surface morphologies upon their tribological properties.

In this study, we perform a novel investigation of arapaima scales. The surface morphologies and tribological properties of the scales were carefully examined. The findings reveal that the surface morphology varies across different regions of the arapaima scale, resulting in significantly different tribological properties. During a predator attack, tribological properties play a crucial role in the interlocking effect realized between adjacent scales; this directly affects the puncture resistance, flexibility, and stability of the arapaima's dermal armor. This work employs a combination of experimental and theoretical analyses to clearly and precisely determine the underlying morphology–tribological property relationships of the arapaima scales and explore their influence upon protection performance. For arapaima, it optimizes the interaction between adjacent scales by carefully regulating the tribological properties of the scales, thereby enhancing the overall performance of the scale armor. Consequently, this study is expected to offer creative design inspiration for the development of personal protective systems.

2 Materials and methods

2.1 Ethics

All animal treatments complied with Chinese law regarding the protection of animals. Ethical approval was provided by the Animal Experimental Ethical Inspection Committee of Tsinghua University.

2.2 Specimens

In this study, a typical arapaima (*Arapaima gigas*) was used as a biological prototype. *Arapaima gigas* is

one of the largest freshwater fish species in the world and is indigenous to the Amazon basin [32]. This species belongs to a resilient lineage of ancient freshwater fish that is believed to have originated approximately 100 million years ago. It possesses a remarkable size, elongated form, and a subtly flattened shape. Its body is adorned with remarkable scales, which are both substantial and rigid, and are firmly set into the surface of its body. The overall coloration of this species exhibits a grey-green hue, with darker tones along the dorsal region, transitioning to a lighter shade towards the ventral region. Moreover, the caudal fin and the posterior portion of the body exhibit a fascinating reddish pigment. A deceased arapaima specimen obtained through legal and ethical channels was used in this study. Following natural death, the arapaima's scales were carefully removed. First, the scales were washed with deionized water and treated with ultrasound for 5 min to remove mucus or contaminants. Next, the scales were immersed in deionized water at room temperature (25 °C) for 4 h. Finally, the scales were allowed to dry naturally for 3 days, and 1.5 kg weights were placed on each scale to prevent curling under surface tension. Adequate ventilation was provided during the drying process. Next, the scales were stored in a freezer at –20 °C until analysis. All biological samples used in this study were obtained from these scales. The scales on the body of the arapaima are arranged in an imbricate pattern, and each individual scale can be divided into an exposed region (black) and a covered region (white).

2.3 Surface morphology observation

The surface morphology of each individual arapaima scale was observed using an ultra-depth-of-field microscope (VHX-6000, Keyence, Japan). Dimensional measurements and statistical analyses were performed using an optical microscope. Parts of a single scale were treated with gold spraying and further examined using electron microscopy (Quanta 200FEG, FEI, the Netherlands). The samples were gold-coated and observed in secondary electron mode at an accelerating voltage of 10 kV. Moreover, the cross-section of a single scale was observed using the ultra-depth-of-field microscope (VHX-6000, Keyence, Japan). Finally, nanoindentation (TI 980, Bruker, USA) testing was performed on the cross-section of a single scale (using a Berkovich tip on the polished flat cross-section), to measure the elastic moduli and hardnesses of the different layers. A maximum force of 50 μN was applied at a loading rate of 50 μN/min.

2.4 Friction detection

Arapaima are frequently targeted by piranhas, whose highly mineralized teeth serve as their primary weapons during attacks and provide a bite force of 0–20 N [4]. However, it is difficult to obtain piranha teeth. Therefore, the present study employed ZrO_2 (a ceramic material commonly used in the production of artificial teeth) to replace piranha teeth in friction wear experiments. The load used in the experiments was set to 10 N. The tribological properties of the arapaima scales were analyzed using a universal mechanical tester tribometer (UMT-5, Bruker, USA) in the reciprocating ball-on-plate mode. The other experimental parameters were as follows: the frequency was set at 1 Hz, the wear track distance was 2.5 mm, and a ZrO_2 ball with a diameter of 12.7 mm was used as the stationary upper counterpart. The water content of the arapaima scale is a critical factor influencing its mechanical properties; hence, the temperature and humidity of the environment were controlled, to maintain a stable scale water content during experiments. To comprehensively analyze the tribological properties of the arapaima scales, experiments were conducted in different regions and orientations. To ensure the accuracy of the experimental results, friction wear measurements were performed at least three times.

Following completion of the friction-wear experiments, the surface morphologies of both the ZrO_2 balls and arapaima scales were observed using the ultra-depth-of-field microscope. Subsequently, the wear tracks of the ZrO_2 balls were determined using a white light interferometer (Nexview NX2, ZYGO, USA). However, because the covered region of the arapaima scales was translucent, the white-light interferometer could not observe the morphology of the scales' translucent regions. To address this, the surface morphology of arapaima scales was observed using the ultra-depth-of-field microscope. In particular, the maximum depths of the wear scars in the middle

(parallel to the reciprocating direction) of the scales were used to characterize the wear rate.

3 Results

3.1 Surface morphology of arapaima scales

Arapaima possesses a distinctive flexible dermal armor that offers excellent protection and flexibility whilst using a limited number of biological components (Fig. 1(a)). The surface of the arapaima is uniformly covered with scales arranged in an imbricate pattern (Fig. 1(b)). Each arapaima scale is elliptical, with an average length and width of 50±10 and 35±8 mm, respectively (Fig. 1(c)). In addition, each scale consists of exposed and covered regions, with the exposed region accounting for ~25% of the total area. The exposed region is black and opaque, whereas the covered region is white and transparent; a clear boundary separates the two regions (Figs. 1(d)–1(f)). Furthermore, the surface morphology of the exposed region is bumpy, whereas that of the covered region is grooved and circular (Figs. 1(g) and 1(h)). The surface morphology of the covered region is also directional. Cross-sectional analysis further revealed that each scale was composed of multiple layers, both external and internal (Fig. 1(i)). As shown in Fig. 2, the elastic modulus and hardness measurements at different positions on the cross-sections of the arapaima scales indicate that these properties decrease from the external to the internal layer; this is appropriate for a multi-layered material structure with a rigid exterior and softer interior. Generally, arapaima scales are multi-layered materials with surface morphologies that vary between different regions, and the covered regions exhibit distinctive directional features. These characteristics are likely to affect the tribological behavior of the scales.

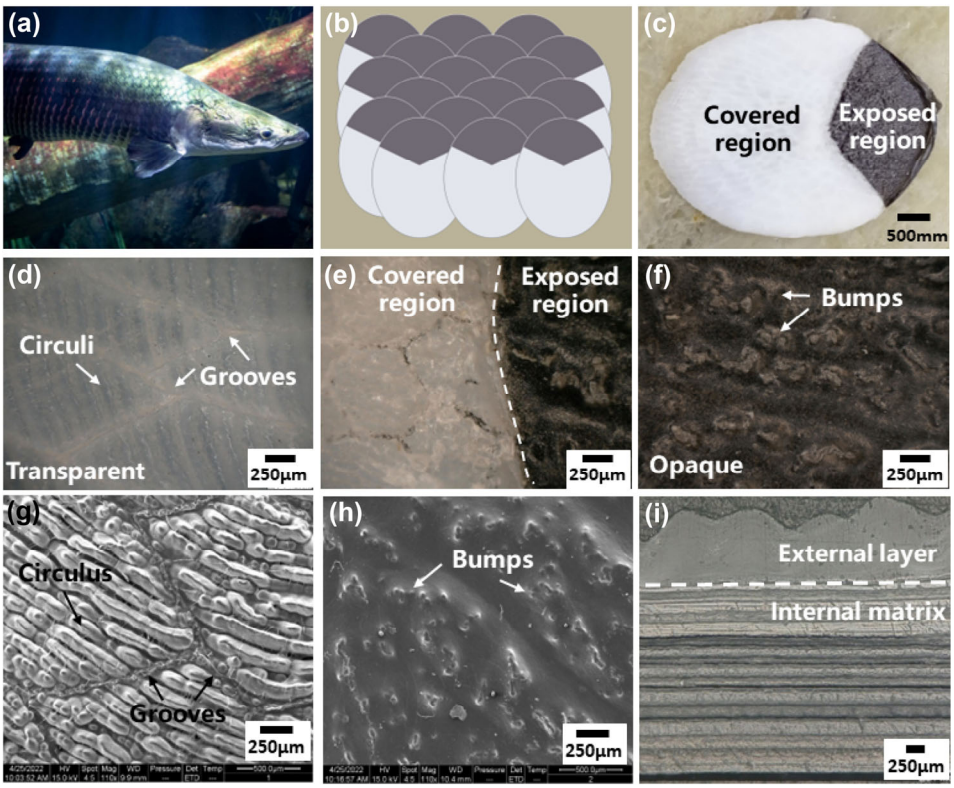

Fig. 1 Surface morphology of arapaima scales: (a) *Arapaima gigas*; (b) Arapaima scales arranged in an imbricate pattern; (c) a single scale, which can be divided into an exposed region (black) and a covered region (white); (d–f) light optical microscopy of single scale in covered, transition, and exposed regions, where the exposed region is opaque, the covered region is transparent, and a clear boundary can be observed in the transition region; (g, h) scanning electron micrographs of different regions: the surface morphology of exposed regions is bumpy, whereas that of covered regions is grooved and circular; and (i) light optical microscopy of the cross-section of a single scale, showing the multilayered material.

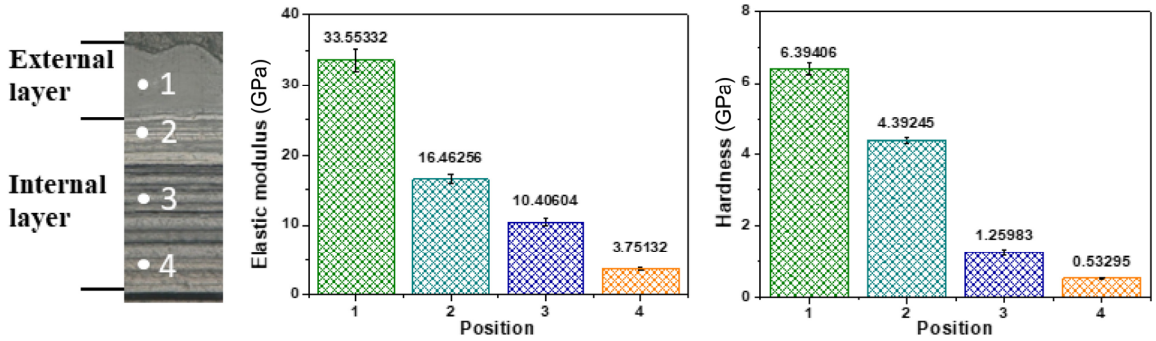

Fig. 2 Elastic modulus and hardness at different positions on the cross-sections of arapaima scales.

3.2 Tribological properties of arapaima scales across different regions

The analysis revealed that the covered and exposed regions of the arapaima scales exhibited distinct surface morphologies, with the covered regions showing significant directional features. These factors are expected to influence the scales' tribological properties. To investigate this, tribological tests were conducted on the covered region along two directions (i.e., along the long and short axes of the scale). Three types of tests were performed according to the different regions and slip directions: LC-type, in which ZrO_2 balls slid along the long axis of scales in the covered region; SC-type, in which ZrO_2 balls slid along the short axis of scales in the covered region; and SE-type, in which ZrO_2 balls slid along the short axis of scales in the exposed region.

As shown in Fig. 3, the friction coefficient varied significantly with respect to sliding time for the different types of tests. Initially, the friction coefficient increased rapidly; this was followed by a slower increase before finally stabilizing. More specifically, the covered region (LC- and SC-type) exhibited a higher friction coefficient, requiring more time to reach a stable value. Conversely, the exposed region (SE-type) exhibited a lower friction coefficient and reached a stable value more quickly. The stable friction coefficients for the LC-, SC-, and SE-type tests were 0.596, 0.560, and 0.392, respectively. To summarize, for the exposed region, the friction coefficient stabilized faster and was lower; in contrast, for the covered region, it took longer to stabilize and yielded a higher friction coefficient. Furthermore, the direction of the surface morphology also affects the friction, with parallel sliding on the long axis resulting in a higher friction coefficient.

In this study, we sought to elucidate the tribological mechanisms of various types of arapaima scales. To achieve this, we analyzed the wear morphology of the contact area after the friction experiment. As shown in Fig. 4, significant wear scars were observed on the surfaces of the ZrO_2 balls after the tribological tests. To perform a detailed analysis of the wear scars, we used a white-light interferometer to obtain their three-dimensional morphologies. The wear scars

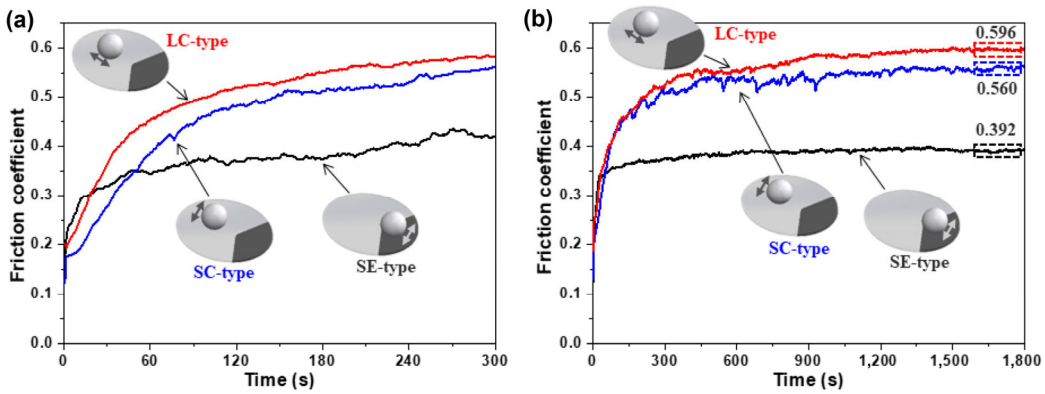

Fig. 3 Variation of friction coefficient under wear durations of different types within (a) 5 and (b) 30 min.

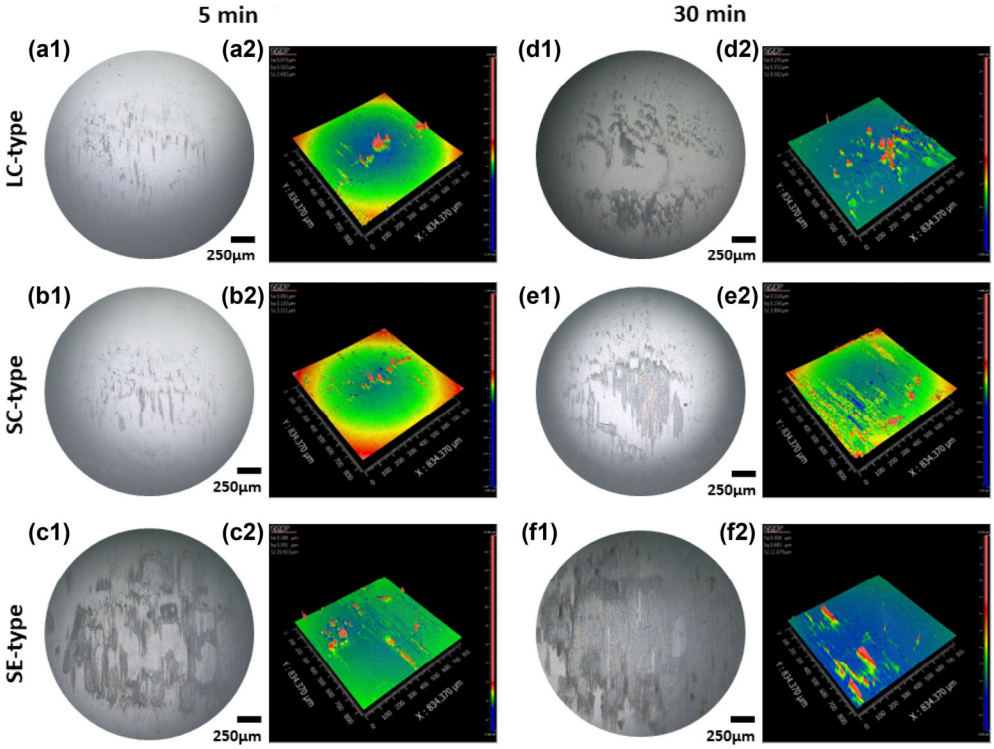

Fig. 4 Morphology of the worn surfaces on ZrO_2 balls: (left) optical images and (right) 3D morphologies of (a–c) LC-type, SC-type, and SE-type, respectively, after 5 min and (d–f) LC-type, SC-type, and SE-type, respectively, after 30 min.

produced obvious bulges on the surfaces of the ZrO_2 balls. ZrO_2 ceramics have a hardness of up to 14 GPa, significantly higher than that of the external layer of arapaima scales [33]. Therefore, the material loss in the wear scars was primarily attributed to the scales, indicating that the transfer films formed in the wear scars were composed of scale materials. Furthermore, when the wear duration was 5 min, the areas of the transfer films on the covered region (LC- and SC-type) were remarkably small; meanwhile, clear transfer films appeared after a wear duration of 30 min. Conversely, in the exposed region (SE-type), noticeable transfer films were formed after 5 min of wear, and the transfer films on the exposed region were significantly larger than those on the covered region after both 5 and 30 min of wear. The formation of transfer films is strongly correlated with both the wear duration and region. The size of the transfer films was also found to have a strong correlation with the friction coefficient of the arapaima scale, where larger transfer films resulted in smaller friction coefficients. Moreover, the transfer films formed faster and were more observable in the exposed region than in the covered one.

Figure 5 shows optical images of the worn scale surfaces under different test types, indicating noticeable wear scars. The external layer of the scales was highly mineralized; this contributed to its hard and brittle mechanical characteristics [2, 9]. Under friction, the surface material of the scales breaks down into wear debris. The specific surface morphology of the scales separates the external layer into numerous independent mineralized units [12, 16]. The independent mineralized units are ground into platforms during friction, and wear debris accumulates between them. When the wear duration was increased, the material loss of the scales also increased, resulting in more pronounced platforms and a greater accumulation of wear debris. Furthermore, the characteristic size of the bumps in the exposed region (SE-type) exceeded that of the grooves and circulus in the covered region (LC- and SC-type). Consequently, the accumulation of wear debris was less apparent, and the platforms were smaller in the exposed region. Moreover, no significant difference in the wear scars was observed between the LC- and SC-type tests; both exhibited wear debris accumulation in the middle of the platform.

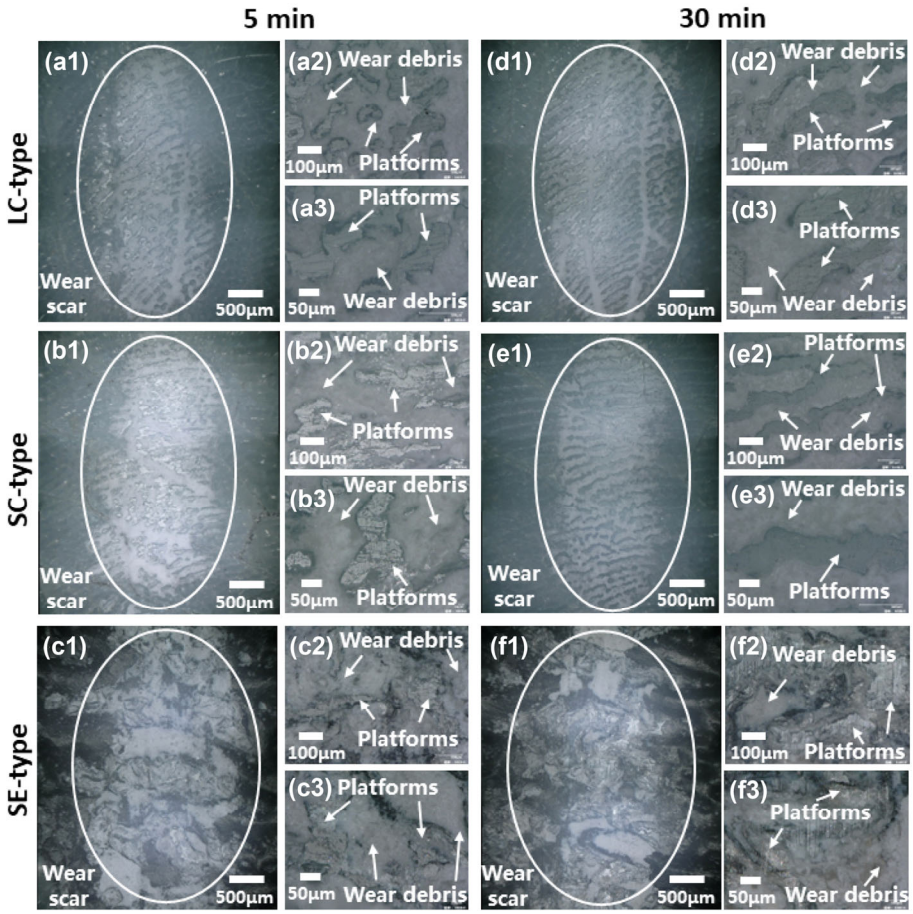

Fig. 5 Optical images of the worn surfaces of arapaima scales under different types of tests: (a–c) LC-type, SC-type, and SE-type, respectively, after 5 min; (d–f) LC-type, SC-type, and SE-type, respectively, after 30 min.

3.3 Wear rate of arapaima scales on different regions

During the initial phase of wear, the wear rate of the scales was low, resulting in a large measurement error. To accurately analyze the wear rates of scales under different sliding conditions, we conducted friction-wear experiments for 180 min under various test types. As shown in Fig. 6, noticeable transfer films were observed on the ZrO_2 balls after 180 min of friction-wear experiments; meanwhile, visible wear scars were present on the surfaces of the arapaima scales. Cross-sectional profiles of the wear scar centers were captured using an ultra-depth-of-field microscope, to assess the wear rate under various test types after 180 min friction-wear experiments. The cross-sectional profiles of the wear scars exhibited a distinctive "U-shape", indicating that the ZrO_2 balls caused significant material removal. In the covered regions (LC- and SC-type), the cross-sectional profiles of the wear scars were smooth. In contrast, the cross-sectional profiles of the wear scars on the exposed region (SE-type) were multimodal. The reasons for these differences are two-fold. First, the grooves and circulus on the covered region were smaller in size, resulting in a larger proportion being removed. Second, the bumps on the exposed region were larger, resulting in a smaller proportion being removed. As shown in Table 1, the maximum wear depths on the wear scars for the LC-, SC-, and SE-type tests were 62.31, 92.97, and 85.81 μm, respectively. It was observed that the sliding direction had a significant effect on the wear rate of the covered region, with a lower wear rate being observed when the sliding direction was parallel to the long axis. Moreover, the wear rate of the covered region exceeded that of the exposed one when the sliding direction was parallel to the short axis.

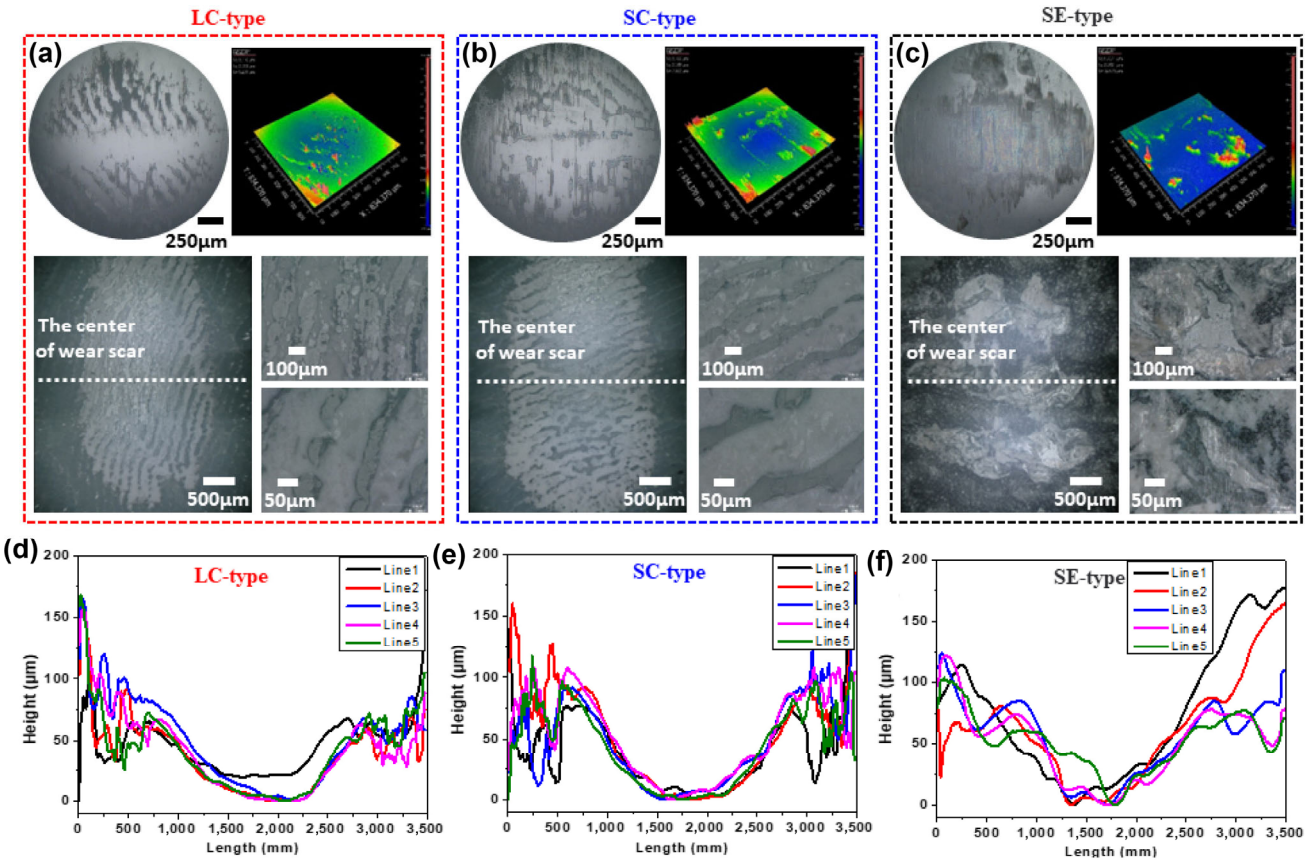

Fig. 6 Worn surfaces on ZrO_2 balls and arapaima scales under different test types after 180 min: (a) LC-type, (b) SC-type, and (c) SE-type. Cross-section profiles of wear scars on scales after 180 min: (d) LC-type, (e) SC-type, and (f) SE-type.

Table 1 Maximum wear depth at the center lines of wear scars after 180 min (unit: μm).

Type	Line1	Line2	Line3	Line4	Line5	Average value	Standard deviation
LC	45.93	60.34	70.29	63.01	72.00	62.31	9.28
SC	76.28	92.61	91.64	107.29	97.03	92.97	10.02
SE	114.03	84.14	85.05	76.32	69.52	85.81	15.20

4 Discussion

4.1 Theoretical explanation

This study aimed to elucidate the tribological properties of arapaima scales in different regions. The difference in tribological properties is generally attributed to the unique surface morphologies of arapaima scales across different regions.

As shown in Fig. 7, for the covered region, the angles between the orientation of the circulus and the sliding direction of the ZrO_2 balls were 45° and 90°, respectively. Previous research has indicated that the mineralized layer of arapaima scales is separated into disconnected mineralized units, and that neighboring units are tethered by fibril bridges [16]. During the friction process, the mineralized units in the arapaima scales underwent elastic deformation until they were broken by the squeezing and rubbing action of the ZrO_2 balls [34–36]. In this process, the relationship between the energy consumed by the arapaima scales (from the ZrO_2 balls) and the wear rate can be expressed as

$$E_k = \xi E_e \tag{1}$$

where E_k is the energy density converted into wear debris, E_e is the energy density absorbed by the scale material, and ξ is the energy conversion coefficient.

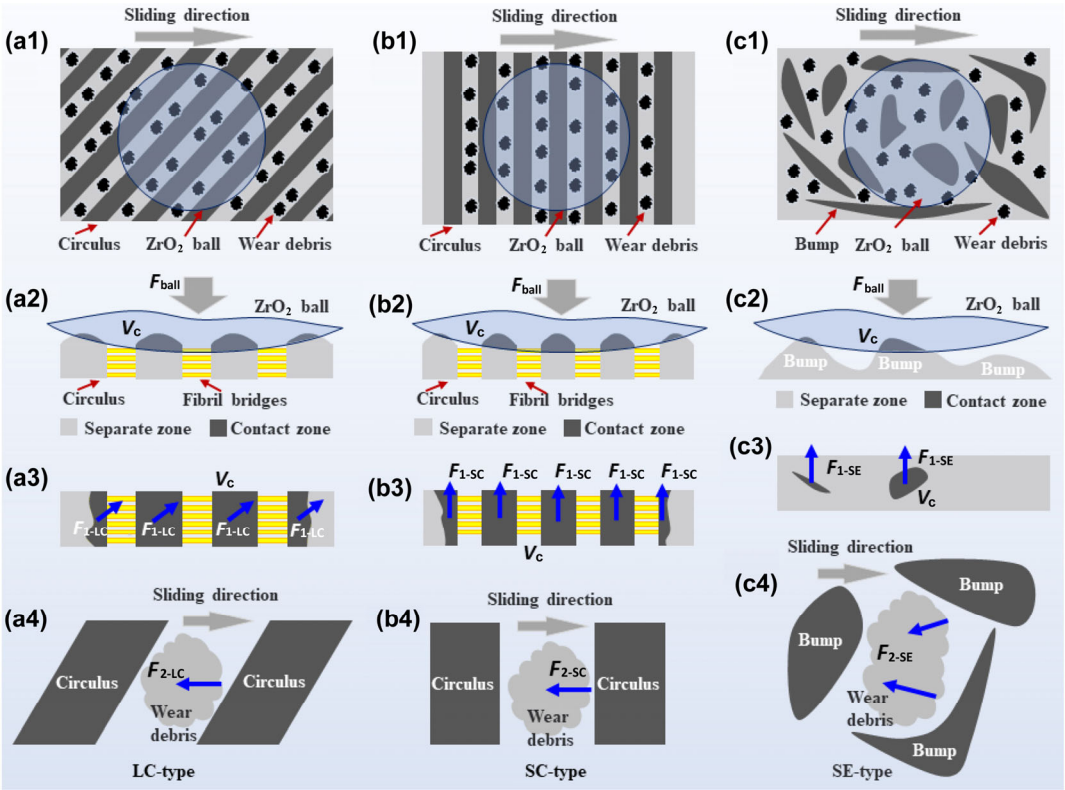

Fig. 7 Theoretical explanation of the tribological properties of arapaima scales under different test types: (a) LC-type, (b) SC-type, (c) SE-type. (a_1–c_1) Top view of the contact between arapaima scales and ZrO_2 balls; (a_2–c_2) cross-section view of the local contact area between arapaima scales and ZrO_2 balls; (a_3–c_3) top view of the local contact area between arapaima scales and ZrO_2 balls; and (a_4–c_4) stress and expansion of wear debris on circulus or bumps.

In the abovementioned process, some of the energy from the ZrO_2 balls was consumed by the fiber bridges. For the LC-type tests, the angle between the fiber bridges and the force ($F_{1\text{-LC}}$) direction of the mineralized units was 45°; in contrast, for the SC-type tests, the angle between the fiber bridges and the force ($F_{1\text{-SC}}$) direction of the mineralized layer units was 90°. Thus, in the LC-type test, fiber bridges could play a more protective role and consume more energy. Consequently, the energy conversion coefficient (ξ) for the LC-type test was smaller, meaning that less energy was used to generate wear debris; this resulted in a lower wear rate [37].

The formation of transfer films on the ZrO_2 balls is an important aspect of the wearing process. The area of the transfer film (S_{tf}) relates to a number of factors:

$$S_{tf} \propto K_1 K_2 K_3 K_4 S_c t \tag{2}$$

Here, S_{tf} denotes the area of the transfer film on the ZrO_2 balls, S_c is the contact area between the ZrO_2 balls and arapaima scales, t is the wear duration, K_1 is a constant related to the properties of ZrO_2 and the arapaima scales, K_2 is a constant pertaining to the experimental environment, K_3 is a constant corresponding to the material removal rate of the arapaima scales, and K_4 is a constant related to the rate at which wear debris adheres to the ZrO_2 balls. On the one hand, for the LC-type test, K_3 is small because of its low wear rate. On the other hand, for the LC-type test, the force ($F_{2\text{-LC}}$) of the wear debris is 45° with circulus; for the SC-type test, the force ($F_{2\text{-SC}}$) of wear debris is 90° with circulus. Therefore, for the LC-type test, wear debris is more easily extended and diffused to both sides; this makes K_4 smaller, meaning that less material is attached to the ZrO_2 balls. In general, for the LC-type test, both K_3 and K_4 are small, leading to a small transfer film area. Consequently, insufficient lubrication during friction leads to higher friction coefficients.

Moreover, the surface morphology of the exposed region is characterized by bumps (Fig. 7(c)); this produces a smaller contact volume between the scales and ZrO_2 balls (compared to the covered region). The relationship between the contact volume and contact stress (between the arapaima scales and ZrO_2 balls) can be expressed as

$$\sigma = F_{ball} / V_c \tag{3}$$

where V_c is the contact volume between the arapaima scales and ZrO_2 balls, F_{ball} is the load of the ZrO_2 balls, and σ is the contact stress between the arapaima scales and ZrO_2 balls. Hence, when a constant force (F_{ball}) was applied, the contact stress of the exposed region was higher, making it easier to remove the material. However, the lacunae created by adjacent bumps can accommodate wear debris (Figs. 5(c)–5(f)). Furthermore, the wear debris fixed in the lacunae was subjected to resistance from the bumps ($F_{2\text{-SE}}$). As a result, the transfer films on the ZrO_2 balls were larger because the expansion of wear debris to the sides was limited, leading to a lower friction coefficient of the exposed region. Furthermore, the transfer films formed rapidly under SE-type conditions. Although the material in the exposed region is initially removed very quickly, the rapid formation of transfer films can reduce the rate of material removal. Therefore, when the sliding direction was parallel to the short axis of the scales, the wear rate of the exposed region was lower than that of the covered region.

4.2 Effects of unique tribological properties of arapaima scales

As shown in Fig. 8, in addition to the fixed force from the flesh (F_F), the imbricated scales experience forces from predator attacks and neighboring scales (F_A, F_B, *a*nd F_C) when attacked by a predator. F_F, F_A, F_B, and F_c are all related to the tribological properties of the arapaima scales; they are the resultant forces of friction (F_{Af}, F_{Bf}, and F_{Cf}) and pressure (F_{Ap}, F_{Bp}, and F_{Cp}). The friction coefficient of the covered region was high, whereas that of the exposed region was low, which affected the values of F_{Af}, F_{Bf}, and F_{Cf}. Consequently, the tribological properties of different regions influence the force received from the predator attack and neighboring scales; this is crucial for protection. The exposed region has a low friction coefficient, which reduces the friction between the predator's body and the scales. When attacked by external objects, the friction coefficient of the scale surface affects its displacement (Δx) and tilt angle

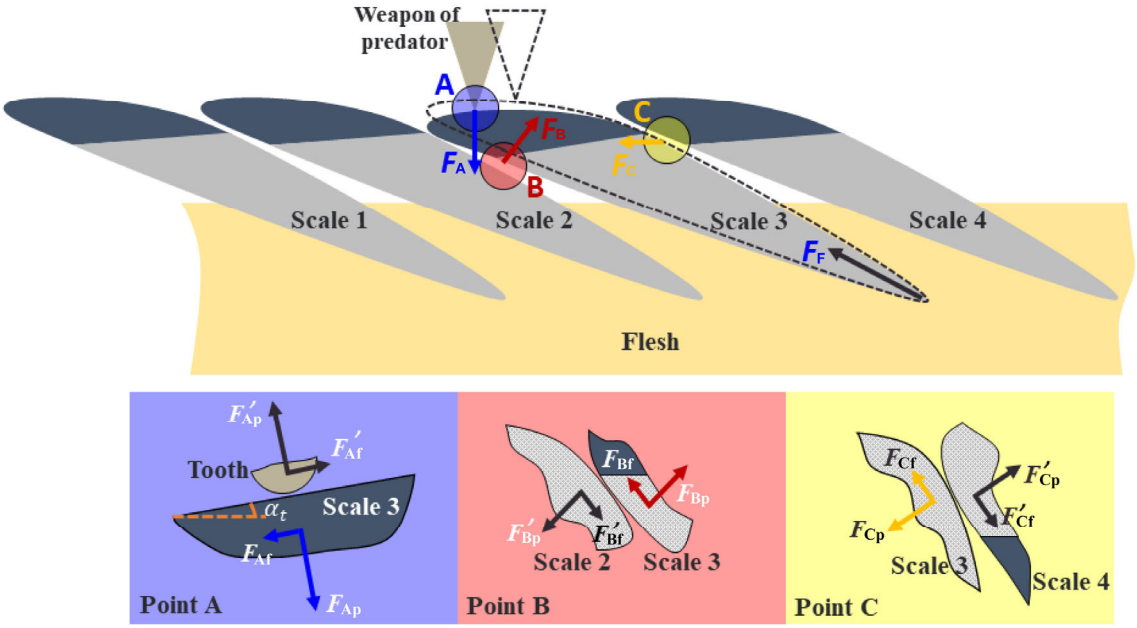

Fig. 8 Effects of tribological properties across different regions.

(α_t), as Eq. (4):

$$\alpha_t \propto \Delta x = F_A / K = \sqrt{F_{Ap}^2 + F_{Af}^2} / K$$

$$= \sqrt{F_{Ap}^2 + (\mu_A F_{Ap})^2} / K \quad (4)$$

Here, α_t is the tilt angle, Δx is the displacement, and K is the elastic modulus of the arapaima scale; μ_A is the friction coefficient of the arapaima scale on the exposed region. The friction coefficient of the exposed region is lower than that of the covered region, and a lower friction coefficient on the exposed region reduces the friction between the predator's body and arapaima scales, resulting in a lower inclination of the scales. The tilt angle of the scales (α_t) is a critical factor in the flexible dermal armor of arapaima, and a high tilt angle is a precursor to failure [30]. Therefore, the low friction coefficient in the exposed region can improve the protective performance of the arapaima. Moreover, a low friction coefficient on the exposed region has other functions; for instance, it can cause slippage of the predator's weaponry and reduce energy consumption when combined with mucus; thus, it plays a protective role [38–42].

The high friction coefficient of the covered region increases the values of F_{Bf} and F_{Cf}. When the arapaima is under attack, the adjacent scales can slide against each other, and the resulting friction can dissipate some of the energy of the attack; this is expressed as

$$E_B = F_{Bf} * d_B = \mu_B F_{Bp} * d_B \quad (5)$$

$$E_C = F_{Cf} * d_C = \mu_C F_{Cp} * d_C \quad (6)$$

where μ_B and μ_C are the friction coefficients of the arapaima scales at Positions B and C, respectively; d_B and d_C are the displacements of the arapaima scales at Positions B and C, respectively; and E_B and E_C denote the energy consumed by the friction of the arapaima scales at Positions B and C, respectively. A high friction coefficient can lead to greater energy consumption when adjacent scales slide directly into each other [43]. As a result, the energy dissipated through the tilt and penetration of scales is reduced, thereby improving puncture resistance. In general, the unique tribological properties across different regions of the arapaima scales play an important role in their resistance to predator attacks. The aforementioned protective strategies serve as a source of inspiration for the advancement of personal protection systems, particularly targeting areas of the body that necessitate flexible movement, such as the neck, elbow, and knee.

5 Conclusions

In this study, we investigated the surface morphologies and tribological properties across different regions of arapaima scales. To summarize, our findings shed light on the characteristics of these regions and contribute to a better understanding of the scales' tribological properties. This study demonstrates that arapaima scales exhibit distinct surface morphologies across different regions. More specifically, the exposed regions of the scales feature grooves and circulus, whereas the covered regions exhibit bumps. The tribological tests conducted in this study disclosed significant differences in the tribological properties of different regions, attributable to the distinct surface morphologies. More specifically, the friction coefficients varied considerably across the different regions, with lower values observed in the exposed region and higher values observed in the covered one. Moreover, the friction coefficient of the arapaima scales in the covered region exhibited directionality with respect to sliding. These findings indicate that the tribological properties of arapaima scales are significantly influenced by their unique surface morphologies. The surface morphologies of arapaima scales can significantly affect the material removal rate, transfer film formation rate, and consequently the friction coefficient and wear rate under different conditions. Consequently, the tribological properties of different regions can influence the forces received from predator attacks and neighboring scales, which are critical factors in the arapaima's protective capabilities. The complex structures of arapaima scales make it difficult to fully understand their properties. Through our investigation, we aim to enhance our understanding of arapaima scales and complement existing biological studies, to yield new insights into the mechanisms of natural flexible dermal armours. Ultimately, the findings of this study offer valuable insights that can contribute to the development of innovative

design concepts for protecting the neck, elbow, and knee—regions that require unrestricted mobility on the battlefield. Consequently, these findings can serve as a catalyst for inspiring fresh approaches in the design of personal protection systems, with the overarching goal of enhancing the effectiveness of battlefield protection for soldiers.

Acknowledgements

This work was financially supported by the National Natural Science Foundation of China (Nos. 52275198, 52205206), and the Opening Project of the Key Laboratory of Bionic Engineering (Ministry of Education), Jilin University (No. K202201).

Declaration of competing interest

The authors have no competing interests to declare that are relevant to the content of this article. The author Prof. Yu TIAN is the Editorial Board Member of this journal.

References

[1] Yang W, Chen I H, Gludovatz B, Zimmermann E A, Ritchie R O, Meyers M A. Natural flexible dermal armor. *Adv Mater* **25**(1): 31–48 (2013)

[2] Yang W, Sherman V R, Gludovatz B, Mackey M, Zimmermann E A, Chang E H, Schaible E, Qin Z, Buehler M J, Ritchie R O, Meyers M A. Protective role of Arapaima gigas fish scales: Structure and mechanical behavior. *Acta Biomater* **10**(8): 3599–3614 (2014)

[3] Zavattieri P D. Tango with the Piranhas. *Matter* **2**(1): 23–25 (2020)

[4] Meyers M A, Lin Y S, Olevsky E A, Chen P Y. Battle in the amazon: Arapaima versus Piranha. *Adv Eng Mater* **14**(5): B279–B288 (2012)

[5] Bezerra W B A, Monteiro S N, Oliveira M S, da Luz F S, Garcia F D, Demosthenes L C D, Costa U O. Processing and characterization of Arapaima gigas scales and their reinforced epoxy composites. *J Mater Res Technol* **9**(3): 3005–3012 (2020)

[6] Estrada S, Munera J C, Hernandez J, Arroyave M, Arola D, Ossa A. Bioinspired hierarchical impact tolerant materials. *Bioinspir Biomim* **15**(4): 046009 (2020)

[7] Chandler M Q, Allison P G, Rodriguez R I, Moser R D, Kennedy A J. Finite element modeling of multilayered structures of fish scales. *J Mech Behav Biomed Mater* **40**: 375–389 (2014)

[8] Lin Y S, Wei C T, Olevsky E A, Meyers M A. Mechanical properties and the laminate structure of Arapaima gigas scales. *J Mech Behav Biomed Mater* **4**(7): 1145–1156 (2011)

[9] Torres F G, De la Torre D, Merino M. Dynamic mechanical analysis of fish dermal armour from A. gigas and P. pardalis. *Bioinspir Biomim Nan* **4**(3): 199–206 (2015)

[10] Gil-Duran S, Arola D, Ossa E A. Effect of chemical composition and microstructure on the mechanical behavior of fish scales from Megalops Atlanticus. *J Mech Behav Biomed Mater* **56**: 134–145 (2016)

[11] Troncoso O P, Gigos F, Torres F G. Mineral and water content of A-gigas scales determine local micromechanical properties and energy dissipation mechanisms. *Mech Time-Depend Mater* **21**(4): 613–625 (2017)

[12] Arola D, Murcia S, Stossel M, Pahuja R, Linley T, Devaraj A, Ramulu M, Ossa E A, Wang J. The limiting layer of fish scales: Structure and properties. *Acta Biomater* **67**: 319–330 (2018)

[13] Drelich A J, Monteiro S N, Brookins J, Drelich J W. Fish skin: A natural inspiration for innovation. *Adv Biosyst* **2**(7): 1800055 (2018)

[14] Torres F G, Le Bourhis E, Troncoso O P, Llamoza J. Structure-property relationships in Arapaima gigas scales revealed by nanoindentation tests. *Polym Polym Compos* **22**(4): 369–373 (2014)

[15] Murcia S, Lavoie E, Linley T, Devaraj A, Ossa E A, Arola D. The natural armors of fish: A comparison of the lamination pattern and structure of scales. *J Mech Behav Biomed Mater* **73**: 17–27 (2017)

[16] Jiang H Y, Ghods S, Weller E, Waddell S, Peng G J, Yang F J, Arola D. Importance of radial line and circulus distributions to the protectoflexibility of scales in fish armors. *Cell Rep Phys Sci* **3**(9): 101022 (2022)

[17] Sherman V R, Quan H C, Yang W, Ritchie R O, Meyers M A. A comparative study of piscine defense: The scales of Arapaima gigas, Latimeria chalumnae and Atractosteus spatula. *J Mech Behav Biomed Mater* **73**: 1–16 (2017)

[18] Zimmermann E A, Gludovatz B, Schaible E, Dave N K N, Yang W, Meyers M A, Ritchie R O. Mechanical adaptability of the Bouligand-type structure in natural dermal armour. *Nat Commun* **4**: 2634 (2013)

[19] Yin S, Yang W, Kwon J, Wat A, Meyers M A, Ritchie R O. Hyperelastic phase-field fracture mechanics modeling of the toughening induced by Bouligand structures in natural materials. *J Mech Phys Solids* **131**: 204–220 (2019)

[20] Pinto F, Iervolino O, Scarselli G, Ginzburg D, Meo M. Bioinspired twisted composites based on Bouligand structures. In Proceedings of the Conference on Bioinspiration, Biomimetics, and Bioreplication, Las Vegas, USA, 2016: 97970E.

[21] Torres F G, Malasquez M, Troncoso O P. Impact and fracture analysis of fish scales from Arapaima gigas. *Mater Sci Eng C-Mater Biol Appl* **51**: 153–157 (2015)

[22] Torres F G, Troncoso O P, Amaya E. The effect of water on the thermal transitions of fish scales from Arapaima Gigas. *Mater Sci Eng C-Mater Biol Appl* **32**(8): 2212–2214 (2012)

[23] Torres F G, Troncoso O P, Nakamatsu J, Grande C J, Gomez C M. Characterization of the nanocomposite laminate structure occurring in fish scales from Arapaima Gigas. *Mater Sci Eng C-Biomimetic Supramol Syst* **28**(8): 1276–1283 (2008)

[24] Murcia S, Li G H, Yahyazadehfar M, Sasser M, Ossa A, Arola D. Effects of polar solvents on the mechanical behavior of fish scales. *Mater Sci Eng C-Mater Biol Appl* **61**: 23–31 (2016)

[25] Liu P, Zhu D J, Yao Y M, Wang J W, Bui T Q. Numerical simulation of ballistic impact behavior of bio-inspired scale-like protection system. *Mater Des* **99**: 201–210 (2016)

[26] Chen A L, Thind K, Demir K G, Gu G X. Modeling bioinspired fish scale designs via a geometric and numerical approach. *Materials* **14**(18): 5378 (2021)

[27] Murcia S, Miyamoto Y, Varma M P, Ossa A, Arola D. Contributions of the layer topology and mineral content to the elastic modulus and strength of fish scales. *J Mech Behav Biomed Mater* **78**: 56–64 (2018)

[28] Zhu D J, Szewciw L, Vernerey F, Barthelat F. Puncture resistance of the scaled skin from striped bass: Collective mechanisms and inspiration for new flexible armor designs. *J Mech Behav Biomed Mater* **24**: 30–40 (2013)

[29] Ghosh R, Ebrahimi H, Vaziri A. Contact kinematics of biomimetic scales. *Appl Phys Lett* **105**(23): 233701 (2014)

[30] Martini R, Balit Y, Barthelat F. A comparative study of bio-inspired protective scales using 3D printing and mechanical testing. *Acta Biomater* **55**: 360–372 (2017)

[31] Rudykh S, Ortiz C, Boyce M C. Flexibility and protection by design: Imbricated hybrid microstructures of bio-inspired armor. *Soft Matte* **11**(13): 2547–2554 (2015)

[32] Luxinger A O, Cavali J, Porto M O, Sales-Neto H M, Lago A A, Freitas R T F. Morphometric measurements applied in the evaluation of Arapaima gigas body components. *Aquaculture* **489**: 80–84 (2018)

[33] Krell A. Load dependence of hardness in sintered submicrometer Al_2O_3 and ZrO_2. *J Am Ceram Soc* **78**(5): 1417–1419 (1995)

[34] Meng Y G, Xu J, Ma L R, Jin Z M, Prakash B, Ma T B, Wang W Z. A review of advances in tribology in 2020–2021. *Friction* **10**(10): 1443–1595 (2022)

[35] Cui S G, Liu Y Z, Wang T, Tieu K, Wang L, Zeng D H, Li Z, Li W. Tribological behavior comparisons of high chromium stainless and mild steels against high-speed steel and ceramics at high temperatures. *Friction* **10**(3): 436–453 (2022)

[36] Zhang X G, Zhang Y L, Jin Z M. A review of the bio-tribology of medical devices. *Friction* **10**(1): 4–30 (2022)

[37] Xu W H, Yu S K, Zhong M. A review on food oral tribology. *Friction* **10**(12): 1927–1966 (2022)

[38] Wainwright D K, Lauder G V. Mucus matters: The slippery and complex surfaces of fish. In *Annual Meeting of the Society-for-Integrative-and-Comparative-Biology (SICB)*, San Francisco, USA, 2018: E443–E443.

[39] Chen L, Qian L M. Role of interfacial water in adhesion, friction, and wear—A critical review. *Friction* **9**(1): 1–28 (2021)

[40] Liu M, Ma L R. Drag reduction methods at solid–liquid interfaces. *Friction* **10**(4): 491–515 (2022)

[41] Kim S J, Kim H N, Lee S J, Sung H J. A lubricant-infused slip surface for drag reduction. *Phys Fluids* **32**(9): 091901 (2020)

[42] Zhang K S, Ma C F, Zhang B C, Zhao B, Wang Q. Numerical simulation study on bionic mucus drag reduction of underwater vehicle. *Int J Fluid Mech Res* **47**(4): 371–385 (2020)

[43] Liu H, Yang B M, Wang C, Han Y S, Liu D M. The mechanisms and applications of friction energy dissipation. *Friction* **11**(6): 839–864 (2023)

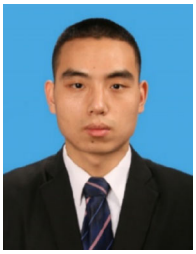

Shuaijun ZHANG. He obtained his Ph.D. degree in bionic science and engineering from Jilin University, China, in 2021. Currently, he is engaged in postdoctoral research at the State Key Laboratory of Tribology in Advanced Equipment at Tsinghua University. His primary research pursuits encompass the fields of biotribology and bionic tribology.

Yu TIAN. He gained his B.S. and Ph.D. degrees in mechanical engineering at Tsinghua University in 1998 and 2002, respectively. His current position is a professor and deputy director of the State Key Laboratory of Tribology in Advanced Equipment (SKLT) at Tsinghua University of China. His research interest is the science and technology at the interface of physics, materials, engineering, and biology, the mechanism of adhesion, friction, and lubrication and their active control.